http://jms.imde.ac.cn

J. Mt. Sci. (2013) 10(5):743-753
DOI: 10.1007/s11629-013-2432-z

Regional Scale Rainfall- and Earthquake-triggered Landslide Susceptibility Assessment in Wudu County, China

BAI Shi-biao, CHENG Chen, WANG Jian*, Benni THIEBES, ZHANG Zhi-gang

College of Geographical Sciences, Key Laboratory of Virtual Geographic Environments (National Education Administration), Nanjing Normal University, Nanjing 210046, China

**Corresponding author: e-mail: wangjian@njnu.edu.cn; Tel: 86-25-85891652; Fax: 86-25-85891347; First author, e-mail: shibiaobai21@163.com*

Abstract: Wudu County in northwestern China frequently experiences large-scale landslide events. High-magnitude earthquakes and heavy rainfall events are the major triggering factors in the region. The aim of this research is to compare and combine landslide susceptibility assessments of rainfall-triggered and earthquake-triggered landslide events in the study area using Geographical Information System (GIS) and a logistic regression model. Two separate susceptibility maps were produced using inventories reflecting single landslide-triggering events, i.e., earthquakes and heavy rain storms. Two groups of landslides were utilized: one group containing all landslides triggered by extreme rainfall events between 1995 and 2003 and the other group containing slope failures caused by the 2008 Wenchuan earthquake. Subsequently, the individual maps were combined to illustrate the locations of maximum landslide probability. The use of the resulting three landslide susceptibility maps for landslide forecasting, spatial planning and for developing emergency response actions are discussed. The combined susceptibility map illustrates the total landslide susceptibility in the study area.

Keywords: Landslides; Susceptibility assessment; Earthquake; Wudu County; China

Introduction

Wudu County is one of the most landslide susceptible regions in China (Scheidegger and Ai 1987). Landslides in Wudu are controlled by environmental conditions, such as weak geological layers, and by strong triggering events, e.g., rainfall and earthquakes. The loose loess deposits and the old landslide bodies exhibit a high permeability while the lower lithological layers consist of less permeable Tertiary and Cretaceous mudstone (Chen 2004). During intensive rainfall events, the water infiltrates directly into the landslide body through cracks, fissures and loess sink holes. Once the water percolates to the material boundary, a plastic flow zone can develop, which significantly decreases slope stability. In the past 10 years, several large landslide events have occurred in the region. The most recent example was the so-called Gansu mudslide, which occurred on August 8, 2010, only 30 km away from the study area. This rainfall-triggered fast-moving debris flow swept through the city, destroyed large areas and claimed at least 1,287 lives (Yu et al. 2010).

Wudu County lies in the north-south seismic region of the Qinghai-Tibet Plateau northern earthquake zone, which has shown recent strong tectonic activity over historic times. Earthquakes with a magnitude greater than 7 have occurred in the study area at least 16 times in written history (Chen 2004). In addition, Wudu County has been greatly affected by the Wenchuan earthquake. Widespread landslides triggered by seismic shaking have been reported by Bai et al. (2010a, 2011). The Wenchuan earthquake caused more than 15,000 landslides, debris flows and rock

Received: 4 June 2012
Accepted: 24 May 2013

avalanches, and it is estimated that approximately 20,000 lives were lost directly due to these landslides (Huang and Li 2008; Cui et al. 2009; Yin et al. 2009; Su et al. 2010; Xu et al. 2011). In addition, the after-effects still threaten the lives of nearly one million people at approximately 12,700 locations throughout the affected area.

In addition to the direct impact of the earthquake, it has also destabilized many slopes and prepared large amounts of material for future landslide events. Consequently, it is estimated that debris flows and landslides will occur at higher intensities and frequencies than normal over the next 5 to 10 years (Tang et al. 2009) or even 10 to 30 years (Cui et al. 2008; Xie et al. 2009). These events can be expected to significantly impact local land use planning and construction and will also restrict future development in the area. To predict the areas that are most likely to experience slope failures in the future, landslide susceptibility maps must be created. Landslide susceptibility is a quantitative or qualitative assessment and classification of the likely spatial distribution of landslides that may occur in an area. Susceptibility may also include a description of the velocity and intensity of the existing or potential landslides (Fell et al. 2008). Both qualitative and quantitative methods have been used to create landslide-susceptibility maps (Aleotti and Chowdhury 1999; Guzzetti et al. 1999). Qualitative methods were widely used during the late 1970s by engineering geologists and geomorphologists. Quantitative methods, however, became popular over the last decades largely because of its numerical expressions of the relationships between controlling factors and landslide events, assisted by the advances in computer and geographic information system (GIS) technology (Guzzetti et al. 2005; van Westen et al. 2008; Sarkar et al. 2008; Pradhan 2010; Wang et al. 2010; Bai et al. 2010b; Ramani et al. 2011; Althuwaynee et al. 2012; Akgun et al. 2012).

Ordinary logistic regression (OLR) has been extensively applied to landslide susceptibility analyses (Atkinson and Massari 1998; Guzzetti et al. 1999; Lee and Min 2001; Dai et al. 2001; Suzen and Doyuran 2004; Ayalew et al. 2005; Can et al. 2005; van den Eeckhaut et al. 2006; Chang et al. 2007; Nefeslioglu et al. 2008; Bai et al. 2010b Bai et al. 2013). The algorithm of logistic regression estimates maximum likelihood after transforming the dependent variable into a logistic variable, which represents the natural log of the likelihood of the dependent variable occurring.

The aim of this research is to compare landslide susceptibility assessments of rainfall-triggered and earthquake-triggered landslide events. The susceptibility maps are combined into one map, describing the maximum likelihood of future landslide occurrences. Subsequently, the potential use of the results of this work for regional landslide hazard and risk management and spatial planning are discussed.

1 Wudu County

Wudu County covers an area of 4,683 km² and is located in southeast Gansu Province, in Northwestern China (Figure 1). The area is located between the Qinghai-Tibet tectonic belt and the Wudu arc structure. The area was strongly

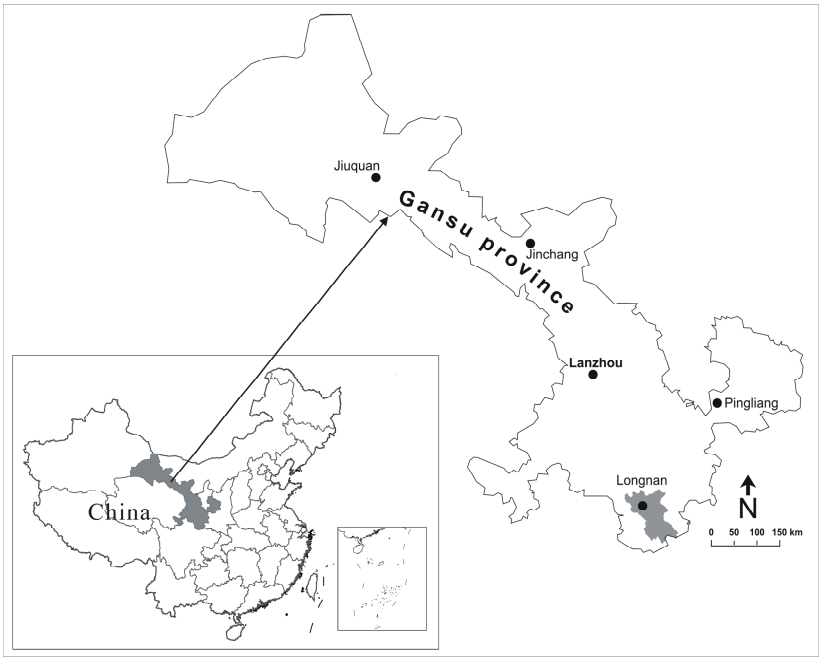

Figure 1 Location of the study area in Wudu county of Gansu province, China

Table 1 Distribution of lithological units in the study area

Lithologic unit	Characteristics
Metamorphic sandstone, metamorphic conglomerate, slate	Metamorphic sandstone, sandy clay slate, sandstone, conglomerate, metamorphic fine sandstone, quartz sandstone
Phyllite, slate, thin limestone	Phyllite mix quartzite, sericite phyllitemix tuff, carbonaceous phyllite mix slate, limestone, chert and fine and siltstone
Thick layer of limestone, slate	Thick layer of limestone rock in the splint, phyllite, chert, silty and fine sand, thick layer of slate, limestone, phyllite, chert and fine and siltstone
Thick layer of sandstone, limestone slate	Thick layer of sandstone, slate phyllite, thin argillaceous limestone
Thick layer of conglomerate, sandy conglomerate	Thick, thick layer of conglomerate, sandy conglomerate mudstones
Siltstone, mudstone, thin sandy conglomerate	Muddy siltstone, silty mudstone in thin muddy sandstone, conglomerate, muddy sandstone
Rock Sand and Gravel	Ancient river bed, modern bed alluvial, alluvial deposits of sand and gravel layers
Magmatic rocks	Granite, diorite, peridotite

influenced by the tectonic uplift of the Qinghai-Tibet plateau, during which strata shifted from a horizontal to a vertical orientation. The geological structures around Wudu are dominated by the southern Qinling fold system. During the geologically recent Yenshan and Himalayan crustal movements, uplift and complex faulting resulted in widespread valley incision and undercutting of the slopes in the region (Derbyshire et al. 1999).

In the study area, a variety of lithological strata are present, including materials from the Silurian, Devonian, Carboniferous, Permian, Triassic, Mesozoic Era and the Quaternary ages.. In particular, the Silurian phyllite, slate and schist are well known for high landslide susceptibility (Li 1997). Based on geological maps at 1:200,000 scale, eight lithological units were defined in which similar materials were grouped according to their composition and physical-mechanical characteristics (Chen et al. 2006) (Table 1). Within each lithological unit, the strata have similar geological properties and conditions. An overview of the eight lithological units is presented in Figure 2.

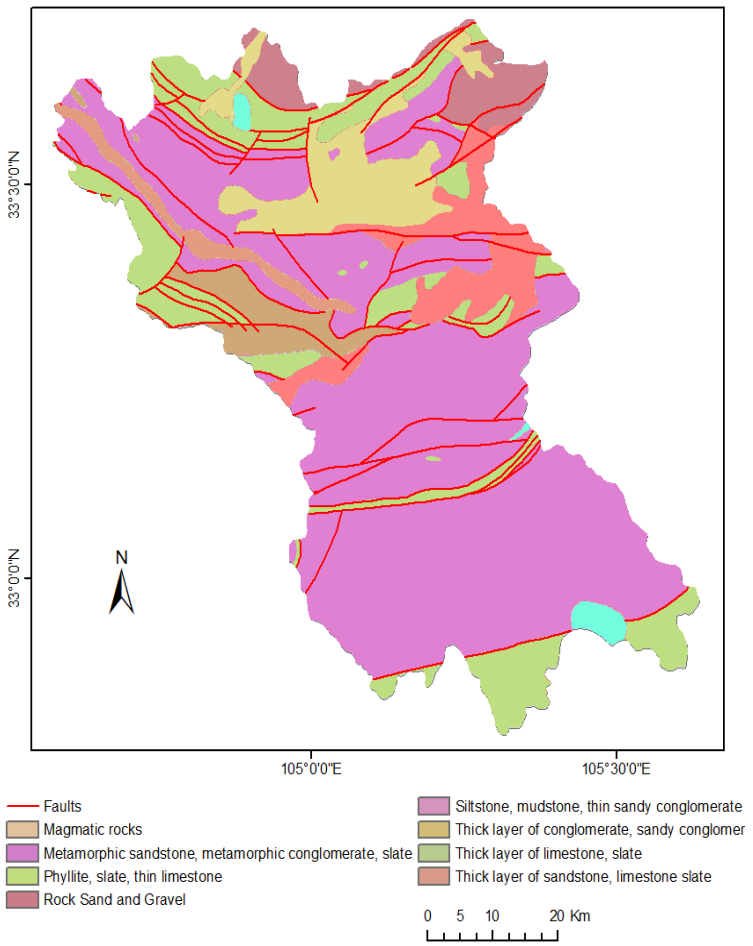

Figure 2 Distribution of lithological units and faults in the study area

Landslides are very common in Wudu County, and slope failures are frequently reported (Chen 2001). Widespread landslide activity was observed particularly in the 1980s. In 1982, 8 times the

typical number of landslides occurred as a consequence of heavy rainstorms in that year. Another significant event occurred on August 3, 1984, when heavy rainfall caused more than 400 debris flows and 570 landslides, which together affected approximately 9.3 million people and caused a direct economic loss of 265.26 million Yuan (approximately 30 million Euro) (Chen 2001).

The most common internationally used landslide classification is from Cruden and Varnes (1996) and is essentially based on material and movement type. According to this classification, the slope failures in Wudu consist of translational and rotational slides which often exhibit a complex flow-like run-out, debris flows, and to a smaller extent rock falls and rock slides. In China, however, a different landslide taxonomy reflecting the material composition and movement categories is acknowledged (Liu and Yan 2002). Within the latter classification, the rainfall-induced landslides in the Wudu region can primarily be classified as colluvial landslides, loess landslides and collapses.

Bai et al. (2012) reported that the statistical analysis of the effect of landslide pre-conditioning factors on distribution and landslide density for earthquake- and rainfall-triggered landslides differ for both the triggering mechanisms. Rainfall-triggered landslides primarily occur on slopes of medium steepness (20-40°). Likewise, for earthquake-triggered landslides, the highest number and density of landslides can be observed for these slopes. However, the majority of seismic landslides can be found in flatter and steeper areas, thus demonstrating a lower influence of slope angle on this type of landslide. No significant differences of landslide distributions for earthquakes of either triggering mechanism were observed for elevation and aspect. The seismic- and rainfall-triggered landslide distributions were found to be similar in terms of the influence of lithology. Both landslide inventories exhibited the highest number of landslides within areas consisting of phyllite, slate and limestone. The highest density of landslides occurred in areas with conglomerates, mudstone and siltstone. The distance to faults was found to strongly control the landslide distributions for both triggering mechanisms.

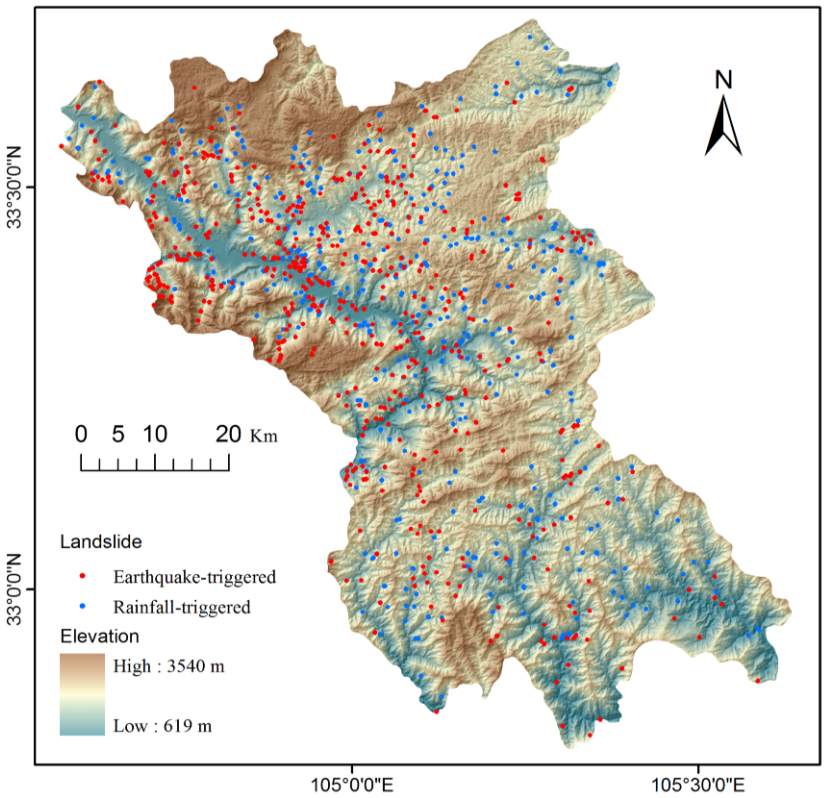

Figure 3 Spatial distribution of rainfall- and earthquake-triggered landslides

2 Input Data

2.1 Landslides inventories

2.1.1 Rainfall-triggered landslides

The Longnan First Station for Landslide and Debris Flow Forecasting and Warning System of the Upper Reaches of the Yangtze River' was created in 1991 and represents the governmental body working on landslides in Wudu county. A research team constructed a historical dataset of rainfall-induced landslides for the study area that covers the period from 1995 to 2003. Within this time period, a total of 505 landslides were reported. (Figure 3)

2.1.2 Wenchuan earthquake-triggered landslides

After the main shock of the Wenchuan earthquake, the 'Ministry of Land and Resources of China' immediately organized scientists to conduct earthquake engineering and geological investigations to provide scientific information in support of decision-making and emergency counter-measures for the immediate post-seismic emergencies, as well as for the mid-term transitional resettlement and reconstruction. To obtain reliable information on the seismogenic geohazards, the investigation applied two approaches: field investigation and remote-sensing image interpretation (Huang and Li 2008; Tang et al. 2009).

The Wenchuan earthquake-triggered landslide dataset contains information from a variety of sources: post-earthquake field investigation, monoscopic manual interpretation of remote-sensing image data (SPOT 5, ALOS and aerial photographs), 1:2,000 digital orthophoto maps (DOM) and a digital elevation model (DEM) with a 30 × 30 m resolution. The landslide morphology recognizable on the available images includes visible scarps, hummocky topography and landslide dams were inventoried and mapped. Landslide types were summarized in terms of the following classes: rockfalls (including rock falls, debris falls and rock avalanches); landslides (debris slides, rotational slides and slumps); and debris flows, according to Cruden and Varnes' (1996) classification. The inventory of earthquake-triggered landslides used within this study is based on the post-seismic emergency reports of the general monitoring station of the geological environment of Gansu Province (Longnan Bureau of Land and Resources, 2008) and the remote sensing emergency survey in the Wenchuan earthquake area (Qin et al. 2009). In total, 555 earthquake-triggered landslides are present in the study area (Figure 2).

2.2 Landslide pre-conditioning factors

The occurrence of landslides is a function of direct and indirect natural conditions and human factors, such as lithology, tectonics, geomorphology, topography, precipitation, temperature, infiltration, runoff, land cover, and road construction (Kamp et al. 2008). These elements are commonly referred to as pre-conditioning factors (Glade and Crozier 2005). To derive the pre-conditioning factors in preparation for the subsequent analysis, several data sources were utilized. These sources include digital orthophotos, and topographical parameters (e.g., altitude, slope, aspect, profile curvature and plan curvature) derived from a digital elevation models (DEM), geology maps (1:200,000), land use maps (1:100,000) and information on road networks and rivers.

The pixel size of the digital elevation model (DEM) is 30 m × 30 m (Figure 3). All other map-based information was transferred to the same pixel size, regardless of the scale of the original source. However, the consequences of this step must be carefully considered in subsequent interpretations. The elevation, slope angle, aspect, plan curvature and profile curvature are derived from the DEM using standard ArcGIS® software, while the distances from slope failures to rivers, roads and faults were measured from the digitized 1:200,000 topographical and geological maps.

The land use data were derived from Landsat TM 5 satellite imagery using various image processing and enhancement techniques (Wu et al. 2004). The analyzed images were then digitally processed to further delineate the boundaries by supervised classification with ERDAS (Earth Resource Data Analysis System) software. The accuracy of the land-use interpretation was validated in the field.

Daily rainfall data from 16 weather stations within and close to the study area were available to this study. The daily rainfall data were utilized to create average annual rainfall contour maps. These maps were then used in a spatial interpolation by Kriging within ArcGIS. An average annual rainfall contour map was created using these recorded precipitation data by a spatial Kriging interpolation (Figure 4).

The triggering factors of earthquake events are related to earthquake intensity. For this study, the Peak Ground Acceleration (PGA) was selected as the main earthquake landslide-triggering factor. PGA data were obtained from the earthquake strong-motion record of the National Strong Motion Observation Network System (NSMONS) (Lu et al. 2010). The NSMONS consists of permanent free-field stations, special observation

arrays, mobile observatories and a network management system. During the Wenchuan earthquake, over 1,400 data points of acceleration records were obtained from 460 permanent free-field stations. In addition, three arrays measuring the topographical effect and the structural response of the main shock were integrated into the network system.

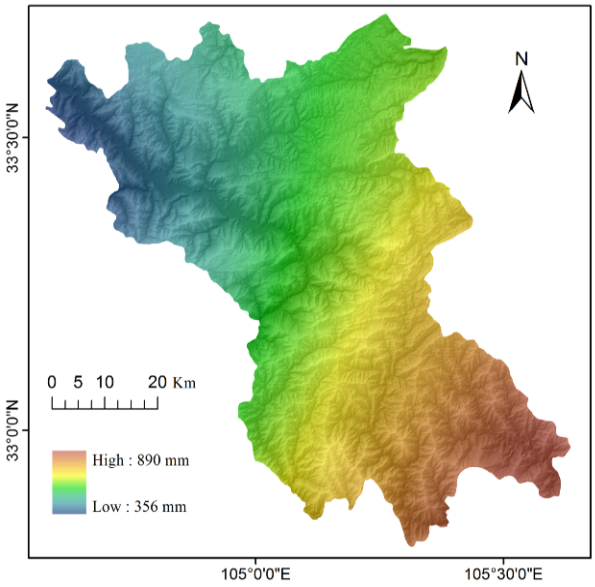

Figure 4 The average annual precipitation based on data from 1971 to 2005

3 Methods

The methodology applied in this study involves a stepwise procedure. In the first step, the influence of preconditioning environmental factors on landslide occurrences is analyzed. In the second step, the landslide susceptibility is mapped by a logistic regression method using each landslide inventory separately, and the results are compared. In the final step, the two landslide susceptibility maps are combined to describe the maximum landslide probability.

3.1 Landslide susceptibility mapping using logistic regression

We applied a logistic regression model to map regional landslide susceptibility. In this study, the dependent variable is a binary variable representing the presence or absence of a landslide. The logistic model can be expressed in its simplest form as:

$$P = \frac{1}{1+e^{-z}} \quad (1)$$

where P is the probability of an event (landslide) occurrence, which ranges from 0 to 1 on an s-shaped curve, and z is defined in the following equation (linear logistic model) with a range from -∞ to +∞:

$$z = \hat{\beta}_o + \hat{\beta}_1 x_1 + \hat{\beta}_2 x_2 + \ldots + \hat{\beta}_n x_n \quad (2)$$

where $\hat{\beta}_0$ is the intercept of the model, n is the number of independent variables, $\hat{\beta}_i$ (i = 1, 2, 3, ..., n) is the slope coefficient of the model, and xi (i = 1, 2, 3, ..., n) are the independent variables. This linear model is a logistic regression representing the presence or absence of landslides (at the present conditions) on the independent variables (pre-failure conditions).

The landslide susceptibility analysis using the logistic regression model includes four main steps: (1) splitting the dataset and resampling, (2) multi-collinearity diagnosis, (3) application of logistic regression model and (4) validation and evaluation of the model results.

In logistic regression, the use of equal numbers of landslide and non-landslide pixels is generally recommended (Süzen and Doyuran 2004; Yesilnacar and Topal 2005; Nefeslioglu et al. 2008), Moreover, approximately 20% of the randomly selected parent data should be used to validate the results (Van Den Eeckhaut et al. 2006). For the Wenchuan earthquake landslide inventory, 555 random sample locations were chosen from the landslide-free area to represent the absence of landslide events. The 555 landslide pixels and 555 landslide-free pixels were merged into a single dataset, and a new binary variable indicating the presence or absence of landslides was added. The set of 1110 pixels was subdivided into calibration and validation data subsets. The calibration dataset contained 80% of the pixels, and the validation set contained the remaining 20% of pixels. The same procedure was performed for the 505 pixels extracted from the rainfall-triggered landslide inventory.

Model fitting via logistic regression is sensitive to collinearities among the independent variables (Hosmer and Lemeshow 1989). Tolerance (TOL)

and the variance inflation factor (VIF) are two important indexes for multicollinearity diagnosis. TOL smaller than 0.2 is an indicator for multicollinearity between independent variables, and TOL smaller than 0.1 suggests serious multicollinearity (Menard 1995).

The validation of the susceptibility maps and the analysis of model performance were carried out by calculating the area under the receiver-operating characteristic (AUROC) curve, which constitutes one of the most commonly used accuracy statistical methods for testing the accuracy of statistical susceptibility maps (Begueria 2006).

To generate class breaks, the standard deviation method was applied using ArcGIS 9.3 tools, dividing the probability map into four susceptibility classes: very low, low, medium and high.

3.2 Combination of susceptibility maps

The two landslide susceptibility scores for each pixel, one derived for the rainfall-triggered landslides, and one for the Wenchuan earthquake-triggered slope failures, were compared. In the first step, the susceptibility classes of the rainfall-triggered landslide susceptibility map were re-coded into numerical values from 1 to 4, representing very low to high susceptibility. Similarly, the Wenchuan earthquake-triggered landslide susceptibility maps were re-classified to values of 10, 20, 30 and 40. In a second step, the two maps were overlain in ArcGIS, and the numerical values were summed. Thus, the codes 14 and 24 indicate that the pixels belonged to the very high rainfall-triggered landslide susceptibility class (code 4), and to the low and very low landslide susceptibility class (code 10 and code 20) from the Wenchuan earthquake-triggered landslide susceptibility map, respectively. Thereby, the combined landslide susceptibility map describes the maximum landslide susceptibility.

4 Results

4.1 Landslide susceptibility assessment

In this study, index values of VIF were found to be less than 2 and higher than 0.4 for the TOL. For the Wenchuan earthquake-triggered landslide distribution, variables such as slope, elevation, lithological unit, land use and peak ground acceleration were selected for statistical significance. For the rainfall-triggered landslide susceptibility distribution, variables such as the average annual precipitation during 1971-2009, aspect, lithological unit, elevation and land use were selected for statistical significance.

The application of the logistic regression model resulted in two landslide susceptibility maps, i.e. for rainfall- and earthquake-triggered slope failures, which are presented in Figure 5. Table 2 shows the distribution of the four susceptibility zones for rainfall-triggered and Wenchuan earthquake landslides.

In general, similar distribution of landslide susceptibility was calculated for both triggering agents. The highest susceptibility classes are located on the lower slopes along the main valleys and in particular the Bailong river valley. The rainfall-triggered landslide susceptibility map (Figure 5a) shows slightly fewer areas of high susceptibility for main valley in the northwestern section of the study area, however, the proportion of this class is very similar to the earthquake-triggered landslide susceptibility map (Figure 5b) with approximately 21%. As a consequence, the areas of high susceptibility are lower for the earthquake-triggered landslide susceptibility map in the southern and eastern parts of the study area.

Table 2 Distribution of susceptibility zones

Susceptibility class	Rainfall-triggered landslide			Wenchuan earthquake-triggered landslide		
	Reclassified cell value	Area covered (%)	Number of landslides (%)	Reclassified cell value	Area covered (%)	Number of landslides (%)
Very low	0 - 0.2002	21.04	1.58	0 - 0.2292	17.86	3.60
Low	0.2002 - 0.4767	30.00	13.41	0.2292 - 0.4676	36.13	18.88
Medium	0.4767 - 0.7532	27.69	38.66	0.4676 - 0.706	24.67	28.96
High	0.7532 - 0.9989	21.27	46.35	0.706 - 0.9945	21.34	48.56

Larger differences between the susceptibility maps can be observed with the classes of very low to medium susceptibility; the proportion of low susceptibility is 6% higher for the earthquake-triggered landslide susceptibility map, while the medium class is about 3% lower. In total, 46% and 49% of rainfall- and earthquake-triggered landslides are in the highest susceptibility class, respectively. For the medium class, the distribution is 39% and 29%, respectively.

The validation of the rainfall-triggered landslide susceptibility maps using prediction rates resulted in a value of 70.2% for landslide and 76% for non-landslide, with an average of 73.2%. A high AUC value of 0.782 was calculated, which indicates a good model performance. For the earthquake-triggered landslide susceptibility map, the prediction rate of the validation dataset was found to be 66% for landslide and 62.65% for non-landslide, with an average value of 64.48%. Again, a high AUC value of 0.725 was obtained.

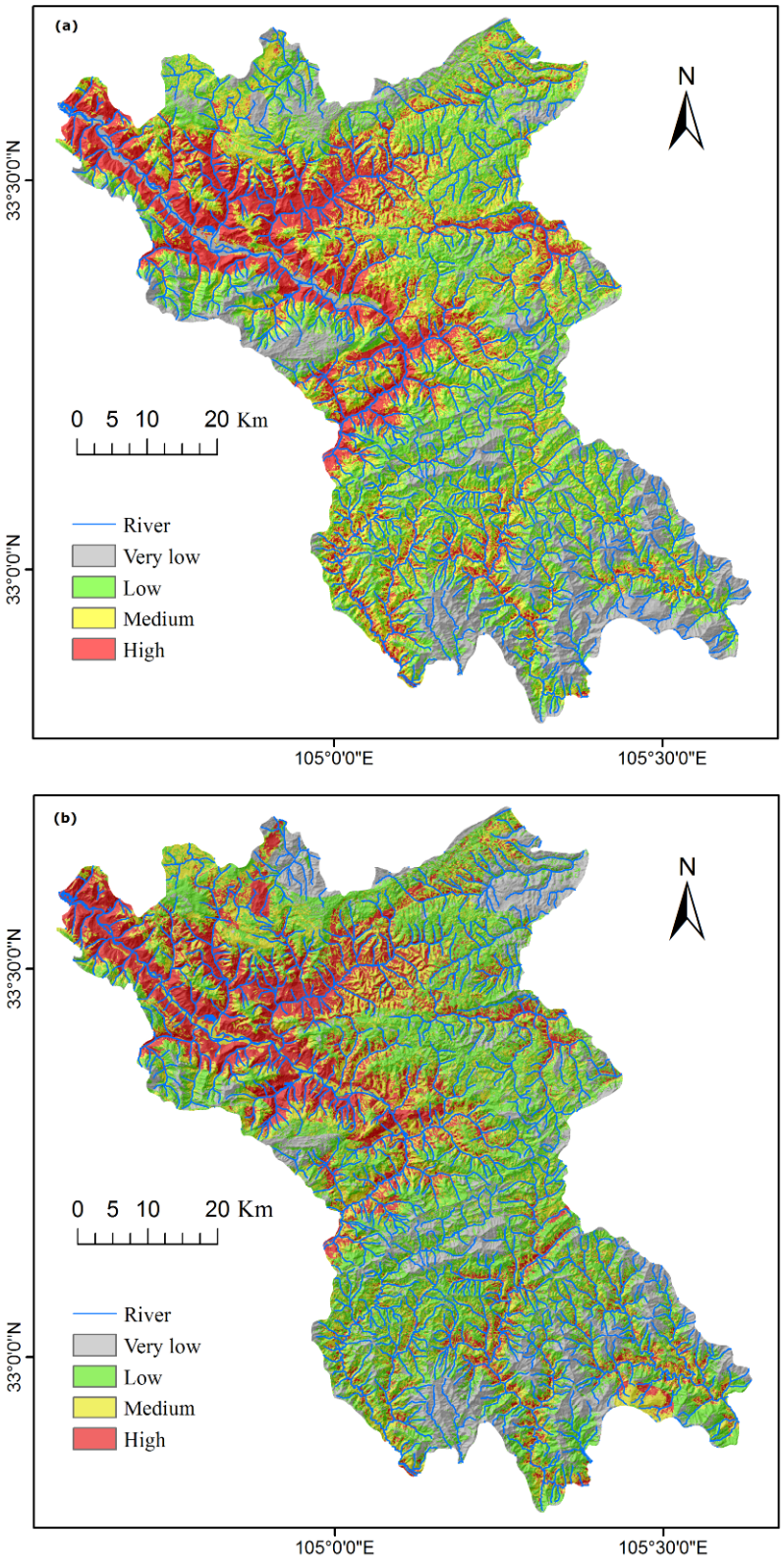

Figure 5 Reclassified susceptibility maps for (a) rainfall-triggered landslides and (b) Wenchuan earthquake-triggered landslides

4.2 Combined landslide susceptibility map

The result of the combination of both susceptibility maps to one maximum susceptibility map (Figure 6). Table 3 gives further details on the distribution of the susceptibility classes within the map. The combined landslide susceptibility map displays the highest susceptibility classes from the two previous maps. Consequently, larger areas than in any of the previous maps are mapped as highly susceptible to failure. Again, the slopes along the major valleys are either classified as high or medium susceptibility areas. In total, approximately 87% of

all landslides are contained in the two highest susceptibility classes, which together make 57% of the study area.

5 Discussion and Conclusion

In this study, we presented a logistic regression model within the GIS framework for landslide susceptibility assessments in an area extremely prone to rainfall- and earthquake-triggered landslides. Separate susceptibility maps were produced for landslides associated with earthquakes and with rainfall. The susceptibility maps were combined into one map describing the maximum likelihood of future landslide occurrences. The prediction capability analysis showed that the two susceptibility maps prepared for rainfall-triggered and earthquake-triggered landslide events both show a wide-spread likelihood of landslide occurrences. In particular along the major valleys are the most densely populated areas. The combined susceptibility map illustrates the total landslide susceptibility in the study area. Despite the fact that large areas have been calculated as highly susceptible to slope failures, less than 50% of the landslides are located in highest susceptibility class, which means, more than half of the landslides are likely to occur in the other areas. This drastically demonstrates the extreme landslide hazards found in the study area.

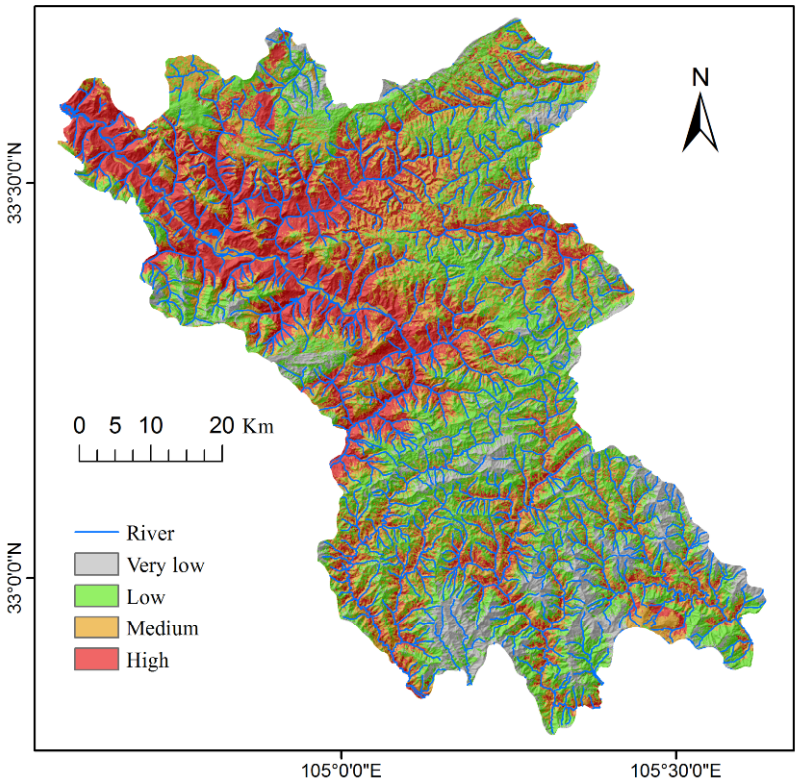

Figure 6 The combined susceptibility map for rainfall- and Wenchuan earthquake-triggered landslide

Table 3 The distribution of combined re-classification susceptibility zones

Susceptibility class	Area covered (%)	Number of landslides (%)
Very low	11.94	1.03
Low	31.28	11.85
Medium	29.48	30.57
High	27.30	56.54

One issue that requires critical discussion is the ability of the results to represent the future distribution of both rainfall- and earthquake-triggered landslides. The susceptibility map created for earthquake-triggered landslide clearly delineates areas which are likely to fail under similar triggering conditions. However, it has to be noted, that future earthquakes are unlikely to produce the same effect as the 2008 Wenchuan earthquake which had a distinct location of epicenter and intensity; the use of a landslide inventory from a different earthquake event would have produced a different susceptibility map. This limitation cannot be avoided without information on landslide distributions caused by other earthquakes. Still, the general trends of landslide susceptibility, which is strongly related to topographical and lithological aspects for both triggering agents, can be considered reliable even though some deviations of future landslide distributions have to be expected.

Landslide susceptibility maps can represent a first stage in the development of landslide hazard or risk zoning for planning purposes (Fell et al. 2008). In our study, large parts of the densely inhabited valleys have been calculated as highly

susceptible to landslides. Due to the fact that the mountainous topography does not allow for a simple selection of safer areas, a general restriction of spatial development in highly susceptible areas cannot be an appropriate option. However, it has to be noted, that the presented study essentially worked on the regional scale, which can not sufficiently include site-specific aspects relevant for landslide triggering. It is therefore recommended to carry out larger scale investigation of the respective slopes including geotechnical investigations, local scale slope stability simulations and landslide run-out modeling, also with respect to different landslide magnitudes. Local and regional decision-makers should be confronted with the scientific results of this study to be able to cooperatively develop appropriate cost-effective counter measure strategies as a part of an integrative risk management. Such counter measures could for example include the promotion of appropriate land-use techniques, the stabilization of slopes with vegetation or engineering solutions, or the installation of landslide forecasting and warning systems. Still, given the extreme landslide hazards in the region, it is impossible to completely avoid landslide-related damage; instead, it is important to understand that living with risk is the only viable solution. Therefore levels of acceptable risks should be determined in collaboration with decision-makers. Then, further studies are required to develop the respective strategies which allow for a cost-effective co-existence with the prevailing hazards.

Acknowledgements

This study was supported by the National Natural Science Foundation of China (Grant No.40930531), the National Key Technology R & D Program (Grant No. 2011BAK12B06), the Opening Fund of State Key Laboratory of Geohazard Prevention and Geoenvironment Protection of Chengdu University of Technology (SKLGP2012K012), the Priority Academic Program Development of Jiangsu Higher Education Institutions, and the 51st Chinese PostDoc Science Foundation (Grant No. 2012M511298). Some of the remote-sensing images were supplied through the ESA-MOST Dragon 3 Cooperation Program (ID: 10606).

References

Akgun A, Sezer EA, Nefeslioglu HA, et al. (2012) An easy-to-use MATLAB program (MamLand) for the assessment of landslide susceptibility using a Mamdani fuzzy algorithm. Computers and Geosciences 38(1):23-34. DOI: 10.1016/j.cageo.2011.04.012

Aleotti P, Chowdhury R (1999) Landslide hazard assessment: summary review and new perspectives. Bulletin of Engineering Geology and the Environment 58: 21-44. DOI: 10.1007/s100640050066

Althuwaynee OA, Pradhan B, Lee S (2012) Application of an evidential belief function model to landslide susceptibility mapping. Computers and Geosciences 44:120-135. DOI: 10.1016/j.cageo.2012.03.003

Atkinson PM, Massari R (1998) Generalized linear modeling of susceptibility to landsliding in the central Apennines, Italy. Computers and Geosciences 24: 373-385. DOI: 10.1016/S0098-3004(97)00117-9

Ayalew L, Yamagishi H, Marui H, et al. (2005) Landslides in Sado Island of Japan Part II. GIS-based susceptibility mapping with comparisons of results from two methods and verifications. Engineering Geology 81: 432-445. DOI: 10.1016/j.enggeo.2005.08.004

Bai SB, Thiebes B, Wang J, et al. (2012) Pre-conditioning factors for rainfall and earthquake-triggered landslides. In: Eberhardt, E. et al. (eds.), Proceedings of the 11th International & 2nd North American Symposium on Landslides. Presented at the Landslides and Engineered Slopes - Protecting Society through Improved Understanding, Taylor & Francis, London, pp 501-505

Bai SB, Wang J, Glade T, et al. (2010a) Comparison on landslide susceptibility assessments before and after 5.12 WenChuan Earthquake at Lognan in China. In: Malet J.P. et al. (eds.), Proceedings of the International Conference Mountain Risks. Bringing Science to Society, Firenze. pp 87-94.

Bai SB, Wang J, Lü GN, et al. (2010b) GIS-based logistic regression for landslide susceptibility mapping of the Zhongxian segment in the Three Gorges area, China. Geomorphology 115: 23-31. DOI: 10.1016/j.geomorph.2009.09.025

Bai SB, Wang J, Zhang ZG et al. (2012) Combined landslide susceptibility mapping after Wenchuan earthquake at the Zhouqu segment in the Bailongjiang Basin, China. Catena 99:18-25. DOI: 10.1016/j.catena.2012.06.012

Begueria S (2006) Validation and evaluation of predictive models in hazard assessment and risk management. Natural Hazards 37(3): 315-329. DOI: 10.1007/s11069-005-5182-6

Chang KT, Chiang SH, Hsu ML (2007) Modeling typhoon-and earthquake-induced landslides in a mountainous watershed using logistic regression. Geomorphology 89: 335-347. DOI: 10.1016/j.geomorph.2006.12.011

Chen YQ (2001) Geo-hazard survey and zone report in Wudu country of Gansu province. Edited by General Monitoring Station of Geological Environment of Gansu province. (In Chinese)

Chen WW, Zhao ZF, Liu G, et al. (2006) The engineering geological problems study of Gansu section of Lanzhou-Haikou highway. Lanzhou: Lanzhou University Press. pp 19-22. (In Chinese)
Cruden DM, Varnes DJ (1996) Landslide types and processes. In: Turner, A.K. et al. (eds.), Landslides: investigation and mitigation. Transp Res Board, Special Report 247, pp 36–75.
Cui P, Wei FQ, He SM, et al. (2008) Mountain Disasters Induced by the Earthquake of May 12 in Wenchuan and the Disasters Mitigation. Journal of Mountain Science 26(3):280-282. (In Chinese) DOI: 10.3969/j.issn.1008-2786.2008.03.006
Cui P, Zhu YY, Han YS, et al. (2009) The 12 May Wenchuan earthquake-induced landslide lakes: distribution and preliminary risk evaluation. Landslides 6: 209-223. DOI: 10.1007/s10346-009-0160-9
Dai FC, Lee CF, Li J, et al. (2001) Assessment of landslide susceptibility on the natural terrain of Lantau Island, Hong Kong. Engineering Geology 40: 381-391. DOI: 10.1007/s00 2540000163
Derbyshire E, Wang JT, Meng XM (1999) The environment: geology. geomorphology, climate and land use. In: Derbyshire, E. et al. (eds.), Landslides in the thick loess terrain of north-west China. pp 22-46.
Fell R, Corornинas J, Bonnard C, et al. (2008) Guidelines for landslide susceptibility, hazard and risk-zoning for land use planning. Engineering Geology 102, 85-98. DOI:10.1016/j.enggeo.2008.03.014
Glade T, Crozier MJ (2005) A review of Scale Dependency in Landslide Hazard and Risk Analysis. In: Glade, T.et al. (eds), Landslide hazard and risk. John Wiley and Sons. pp 75-138.
Guzzetti F, Carrara A, Cardinali M, Reichenbach P (1999) Landslide hazard evaluation: a review of current techniques and their application in a multi-scale study, central Italy. Geomorphology 31: 181-216. DOI: 10.1016/S0169-555X(99)00078-1
Guzzetti P, Reichenbach M, Cardinali M, et al. (2005) Landslide hazard assessment in the Staffora basin, northern Italian Apennines. Geomorphology 72: 272-299. DOI: 10.1016/j.geomorph.2005.06.002
Hosmer DW, Lemeshow S (1989) Applied Regression Analysis.Wiley, New York. pp 307.
Huang RQ, Li WL (2008) Development and distribution of geohazards triggered by the 5.12 Wenchuan Earthquake in China. Science China Ser E-Tech 52(4): 810-819. DOI: 10.1007/s11431-009-0117-1
Kamp U, Growley BJ, Khattak GA, et al. (2008) GIS-based landslide susceptibility mapping for the 2005 Kashmir earthquake region. Geomorphology 101: 631-642. DOI: 10.1016/j.geomorph.2008.03.003
Lee S, Min K (2001) Statistical analysis of landslide susceptibility at Yongin, Korea. Engineering Geology 40: 1095-1113. DOI: 10.1007/s002540100310
Li SD (1997) Discussion on landslide activities in Bailong River basion of Wudu. Bulletin of Soil and Water Conservation 17(6):28-32. (In Chinese)
Liu GR, Yan EC (2002) Discussion on classification of landslides. Journal of Engineering Geology 10(4): 339-342. (In Chinese)
Longnan bureau of land and resources (2008) The recovery and reconstruction of geological disaster prevention special plan at Longnan of Gansu Province. (In Chinese).
Lu DL, Cui JW, Li XJ, et al. (2010) Ground motion attenuation of Ms 8.0 Wenchuan earthquake. Earthquake Science 23: 95-100. DOI: 10.1007/s11589-009-0047-9
Menard SW (1995) Applied Logistic Regression Analysis. SAGE Publication, Inc., Thousand Oaks, CA.
Nefeslioglu HA, Duman TY, Durmaz S (2008) Landslide susceptibility mapping for a part of tectonic Kelkit Valley (Eastern Black Sea region of Turkey). Geomorphology 94: 410-418. DOI: 10.1016/j.geomorph.2006.10.036
Pradhan B (2010) Application of an advanced fuzzy logic model for landslide susceptibility analysis. International Journal of Computational Intelligence Systems, 3(3):370-381. DOI: 10.1080/18756891.2010.9727707
Qin XW, Yang JZ, Zhang Z, et al. (2009) Remote sensing emergency survey in Wenchuan earthquake area. science press of China. pp 285. (In Chinese).
Ramani SE, Pitchaimani K, Gnanamanickam RV (2011) GIS based landslide susceptibility mapping of Tevankarai Ar sub-watershed, Kodaikkanal, India using binary logistic regression analysis, Journal of Mountain Science 8(4):505-517. DOI: 10.1007/s11629-011-2157-9
Sarkar S, Kanungo DP, Patra AK, et al. (2008) GIS based spatial data analysis for landslide susceptibility mapping, Journal of Mountain Science 5(1):52-62. DOI: 10.1007/s11629-008-0052-9
Su FH, Cui P, Zhang JQ, Xiang LZ (2010) Susceptibility assessment of landslides caused by the wenchuan earthquake using a logistic regression model, Journal of Mountain Science7(3): 234-245. DOI: 10.1007/s11629-010-2015-1
Süzen ML, Doyuran V (2004) A Comparison of the GIS based landslide susceptibility assessment methods: multivariate versus bivariate. Environmental Geology 45: 665-679. DOI: 10.1007/s00254-003-0917-8
Tang C, Zhu J, Liang JT (2009) Emergency assessment of seismic landslide susceptibility: a case study of the 2008 Wenchuan earthquake affected a rea, Earthquake Engineering and Engineering Vibration 8: 207-217. DOI: 10.1007/s11803-009-9025-4
Van Den Eeckhaut M, Vanwalleghem T, Poesen J, et al. (2006) Rediction of landslide susceptibility using rare events logistic regression: a case-study in the Flemish Ardennes (Belgium). Geomorphology 76: 392-410. DOI: 10.1016/j.geomorph.2005.12.003
Van Westen CJ, Castellanos E, Kuriakose SL (2008) Spatial data for landslide susceptibility, hazard, and vulnerability assessment: An overview. Engineering Geology 102: 112-131. DOI: 10.1016/j.enggeo.2008.03.010
Wang M, Qiao JP, He SM (2010) GIS-based earthquake-triggered landslide hazard zoning using contributing weight model, Journal of Mountain Science, 7(4):339-352. DOI: 10.1007/s11629-010-2054-7
Wu LX, Sun B, Zhou SL, et al. (2004) A new fusion technique of remote sensing images for land use/cover. Pedosphere 14:187-194.
Xie H, Zhong DL, Jiao Z, et al. (2009) Debris Flow in Wenchuan Quake-hit Area in 2008. Journal of Mountain Science 27(4): 501-509. (In Chinese)
Xu Q, Zhang S, Li WL (2011) Spatial distribution of large-scale landslides induced by the 5.12 Wenchuan Earthquake, Journal of Mountain Science 8(2): 246-260. DOI: 10.1007/s11629-011-2105-8
Yesilnacar E, Topal T (2005) Landslide susceptibility mapping: A comparison of logistic regression and neural networks methods in a medium scale study, Hendek region (Turkey) Engineering Geology 79: 251-266. DOI: 10.1016/j.enggeo.2005.02.002
Yin YP, Wang FW, Sun P (2009) Landslide hazards triggered by the 2008 Wenchuan earthquake, Sichuan, China. Landslides 6: 139-152. DOI: 10.1007/s10346-009-0148-5
Yu B, Yang YH, Su YC, et al. (2010) Research on the giant debris flow hazards in Zhouqu county, Gansu province on August 7, 2010. Journal of Engineering Geology 18(4): 437-444. (In Chinese)